J Electr Eng Technol.2018; 13(1): 256-262
http://doi.org/10.5370/JEET.2018.13.1.256

ISSN(Print) 1975-0102
ISSN(Online) 2093-7423

A Novel Soft Switching PWM·PFC AC·DC Boost Converter

Yakup Sahin†

Abstract – This study introduces a novel Soft Switching (SS) Pulse Width Modulated (PWM) AC−DC boost converter. In the proposed converter, the main switch is turned on with Zero Voltage Transition (ZVT) and turned off with Zero Current Transition (ZCT). The main diode is turned on with Zero Voltage Switching (ZVS) and turned off with Zero Current Switching (ZCS). The auxiliary switch is turned on and off with ZCS. All auxiliary semiconductor devices are turned on and off with SS. There is no extra current or voltage stress on the main semiconductor devices. The majority of switching energies are transferred to the output by auxiliary transformer. Thus, the current stress of auxiliary switch is significantly reduced. Besides, the proposed converter has simple structure and ease of control due to common ground. The theoretical analysis of the proposed converter is verified by a prototype with 100 kHz switching frequency and 500 W output power. Furthermore, the efficiency of the proposed converter is 98.9% at nominal output power.

Keywords: Soft switching, Power factor correction, Zero voltage transition, Zero current transition

1. Introduction

Energy efficiency is becoming more important every day because nonlinear loads and the power electronics converters draw harmonic currents. These harmonics cause corruptions on devices which connected to the grid. The manufacturers should provide international mandatory standards about harmonics and power factor in terms of the use of energy efficiency. The boost converters often used on high frequency AC−DC Power Factor Correction (PFC) applications. The modern PFC converters reduce both reactive power and Total Harmonic Distortion (THD).

The switching frequency of converter should be increased for obtain a high power factor and power density. However, the switching power losses and Electro Magnetic Interference (EMI) occurs on high switching frequency. To overcome these problems, the Soft Switching (SS) converters should be used instead of Hard Switching (HS) converters [1-4].

Zero Voltage Transition (ZVT) and Zero Current Transition (ZCT) techniques are called modern SS techniques. Although the main switch is turned on with ZVT, the auxiliary switch is turned off with HS in the conventional ZVT converter [5]. To overcome the issue of conventional ZVT converter, a lot of snubber cells are introduced in the literature [6-14].

In [6], the main switch is turned on with ZVT and turned off with Zero Voltage Switching (ZVS). But, the current stress occurs on the main switch and auxiliary diode has voltage stress in this converter. A coupled inductor is used in the snubber cell in [7], it ensures ZVT turning on and ZVS turning off for the main switch.

Both of SS techniques ZVT and ZCT are used in [8] for turning on and turning off of the main switch, respectively. Besides, the main diode is turned off with zero current switching (ZCS) and turned on with ZVS. But, the extra current stress occurs on the main switch. In [9,10], all semiconductor devices operate with ZVS or ZCS. However, the operating of converter at light loads is poor.

The oscillation between parasitic capacitance of the main switch and the snubber inductance causes to EMI when the main switch is turned off in [11]. The extra conduction power losses occur since the auxiliary element is on the main current line in [12] and the turning on with ZVT for the main switch is poor at light loads in [13]. The snubber cell has two auxiliary switches and these switches do not have common ground, where the control of converter is difficult in [14]. The main switch is turned off with ZCT in the conventional ZCT converter [15]. However, the turning on of the main switch and the turning off both the main diode the auxiliary switch is with HS. Also, the reverse recovery losses of the main diode are high.

The best solution for eliminating switching power losses is using both ZVT and ZCT techniques simultaneously [16-21]. Here, the main switch turns on with ZVT and turns off with ZCT. However, there are some drawbacks in these converters. In [16], the auxiliary switch and auxiliary diode turns off with hard switching (HS). Therefore, the switching power losses occur on the auxiliary devices. In [17,18], there is high current stress on the main devices and this case leads additional conduction losses. In [19], there is extra voltage stress on the auxiliary switch and diode. In [20], there is extra voltage stress on the main diode and the snubber cell has complex structure. In [21], the tight coupled inductor is required to prevent the losses of the leakage inductance.

† Corresponding Author: Dept. of Electrical and Electronic Engineering, Bitlis Eren University, Turkey. (ysahin@beu.edu.tr)
Received: February 3, 2017; Accepted: September 26, 2017

In this study, a novel soft switching PWM–PFC AC–DC boost converter is proposed to solve drawbacks in previously proposed SS PFC converter. The proposed converter is presented with simulation results as a paper conference in [22]. This study is the extended version of the conference paper along with detailed mathematical analysis, experimental results, the efficiency analysis etc. In the proposed converter, the main switch is turned on with ZVT and turned off with ZCT. The main diode is turned on with ZVS and turned off with ZCS. The auxiliary switch is turned on and off with ZCS. Besides, there is no additional voltage or current stress on the main semiconductor devices and the converter operates a wide line voltage range.

2. Operating Stages and Analysis

2.1 Definitions and assumptions

The proposed converter is presented in Fig. 1. In the main circuit, V_i is input voltage source, V_O is output voltage, L_F is input filter inductance and C_F represents the output filter capacitance. D_F is main diode, S_1 represents main switch and D_1 is its body diode, and also R_L is the resistive load. In the proposed snubber cell, the auxiliary switch is indicated by S_2, the resonance capacitance is denoted by C_S and the resonance inductance is indicated by L_r, while the auxiliary diodes are indicated by D_2, D_3 and D_4. L_m is magnetization inductance, L_{P1} is leakage inductance of primary and L_{S1} is leakage inductance of secondary, 1:a=N_1:N_2 is turns ratio of auxiliary transformer, respectively.

In the steady state analysis of the proposed converter, the following assumptions are considered:

- Filter inductance L_F is assumed to be large enough to keep the input current constant and output filter capacitance C_F is assumed to be large enough so that output voltage can be kept constant.
- The resonance circuits and semiconductor components are ideal.
- Reverse recovery time of all the diodes is ignored.

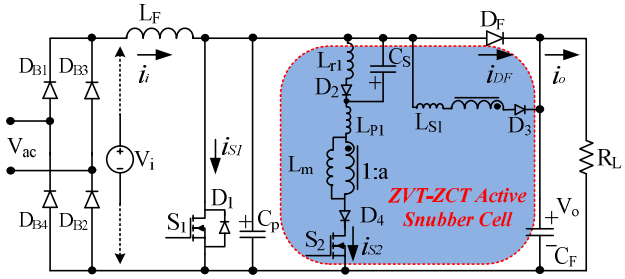

Fig. 1. Proposed novel soft switching PWM-PFC AC-DC boost converter

2.2 Operating stages

The steady state operation of the converter contains eleven operational stages in one switching cycle. The equivalent circuits of these operational stages are presented in Fig. 2. Furthermore, the key waveforms of the operational stages are described in Fig. 3.

Stage 1 [$t_0 < t < t_1$: Fig. 2(a)]

Before $t = t_0$, the switches S_1 and S_2 are in the off–state. The main diode D_F conducts the input current I_i. $i_{S1} = 0$, $i_{DF} = I_i$, $i_{S2} = 0$, $v_{CS} = V_{CS0}$ and $v_{Cp} = V_o$ are valid. At $t = t_0$, the control signal is applied to the gate of auxiliary switch and this stage is started. Then, the main diode current decreases while the auxiliary switch current increases and the voltage of snubber capacitor decreases. Fallowing equations are can be written for this stage:

$$v_{CS} = V_{CS0}\cos\left(\omega_1\left(t-t_0\right)\right) \tag{1}$$

$$i_{Lr2} = \frac{V_{CS0}}{\omega_1 L_{r2}^{\ 2}}\sin\left(\omega_1\left(t-t_0\right)\right) \tag{2}$$

$$i_{D3} = i_{Lr2}\frac{aL_m}{L_m + a^2 L_{sl}} \tag{3}$$

$$L_{r2} = L_{pl} + \frac{L_m a^2 L_{sl}}{L_m + a^2 L_{sl}} \tag{4}$$

$$\omega_1 = \frac{1}{\sqrt{L_{r2}C_S}} \tag{5}$$

At $t=t_1$, the main diode current falls zero when the auxiliary switch current reaches input current I_i. So, the auxiliary switch S_2 is turned on and the main diode D_F is turned off with ZCS due to series inductor L_{r2}.

Stage 2 [$t_1 < t < t_2$: Fig. 2(b)]

In this stage, a resonance begins via $C_p - C_s - L_{r2}$. Thus, the voltage of C_p decreases while the auxiliary switch current is increasing. In here, the energy of C_p is transferred to the transformer. After that, the transformer transfers the majority of this energy to the output side. The energy is transferred to the output during first two stages. In this way, Direct Power Transfer (DPT) can be ensured during these stages. For this stage fallowing equations are valid:

$$L_{r2}\frac{di_{Lr2}}{dt} = V_{Cp} + V_{Cs} \tag{6}$$

$$C_S\frac{dv_{CS}}{dt} = i_{Lr2} \tag{7}$$

$$C_p\frac{dv_{Cp}}{dt} = I_i - i_{Lr2}\left(1 - \frac{aL_m}{L_m + a^2 L_{sl}}\right) \tag{8}$$

At $t = t_2$, D_1 diode turns on with ZVS when the voltage of C_p falls to zero and this stage ends.

Stage 3 [$t_2 < t < t_4$: Fig. 2(c)]

At $t = t_2$, a new resonance starts via $L_{r1} - L_{r2} - C_s$ and the energy of the transformer primary inductance is transferred to L_{r1} and C_s. It is called ZVT stage where D_1 is in the on−state. The control signal is applied to the gate of the main switch S_1 in this stage. In this way, the main switch is turned on with ZVT.

At $t = t_3$, the current of transformer primary inductance falls I_i and D_1 diode turns off with ZCS. After that, the current of the main switch increases while current of transformer primary inductance decreases. In here, the resonant inductance current i_{Lr1}, i_{Lr2} and the resonant capacitor voltage v_{CS} can be expressed as follows:

$$v_{CS} = V_{CS2}\cos\left(\omega_e\left(t-t_2\right)\right) + Z_e\left(I_{Lr22} - I_{Lr12}\right)\sin\left(\omega_e\left(t-t_2\right)\right) \tag{9}$$

$$\begin{aligned} i_{Lr1} &= \frac{L_e}{L_{r1}} I_{Lr22}\left(1-\cos\left(\omega_e\left(t-t_2\right)\right)\right) \\ &+ \frac{L_e}{L_{r2}} I_{Lr12}\left(1-\cos\left(\omega_e\left(t-t_2\right)\right)\right) \\ &+ I_{Lr12}\cos\left(\omega_e\left(t-t_2\right)\right) - \frac{V_{CS2}}{\omega_e L_{r1}} I_{Lr12}\sin\left(\omega_e\left(t-t_2\right)\right) \end{aligned} \tag{10}$$

$$\begin{aligned} i_{Lr2} &= \frac{L_e}{L_{r1}} I_{Lr22}\left(1-\cos\left(\omega_e\left(t-t_2\right)\right)\right) \\ &+ \frac{L_e}{L_{r2}} I_{Lr12}\left(1-\cos\left(\omega_e\left(t-t_2\right)\right)\right) \\ &+ I_{Lr22}\cos\left(\omega_e\left(t-t_2\right)\right) - \frac{V_{CS2}}{\omega_e L_{r2}} I_{Lr12}\sin\left(\omega_e\left(t-t_2\right)\right) \end{aligned} \tag{11}$$

$$L_e = \frac{L_{r1}L_{r2}}{L_{r1}+L_{r2}} \tag{12}$$

$$\omega_e = \frac{1}{\sqrt{L_e C_S}} \tag{13}$$

$$Z_e = \sqrt{\frac{L_e}{C_S}} \tag{14}$$

In here, I_{Lr12} and I_{Lr22} are the values of I_{Lr1} and I_{Lr2} at the end of Stage 2.

At $t = t_4$, the current of transformer primary inductance falls zero when the current of main switch reaches input current value. Therefore, the auxiliary switch turns off with ZCS and this stage ends.

Stage 4 [$t_4 < t < t_5$: Fig. 2(d)]

During this stage, the energy stored in the snubber inductance L_{r1} is transferred to capacitor C_s via $L_{r1}-C_s-D_2$ resonance. For this stage equations are valid:

$$v_{CS} = V_{CS4}\cos\left(\omega_2\left(t-t_4\right)\right) + Z_1 I_{Lr14}\sin\left(\omega_2\left(t-t_4\right)\right) \tag{15}$$

$$i_{Lr1} = I_{Lr14}\cos\left(\omega_2\left(t-t_4\right)\right) + \frac{V_{CS4}}{Z_1}\sin\left(\omega_2\left(t-t_4\right)\right) \tag{16}$$

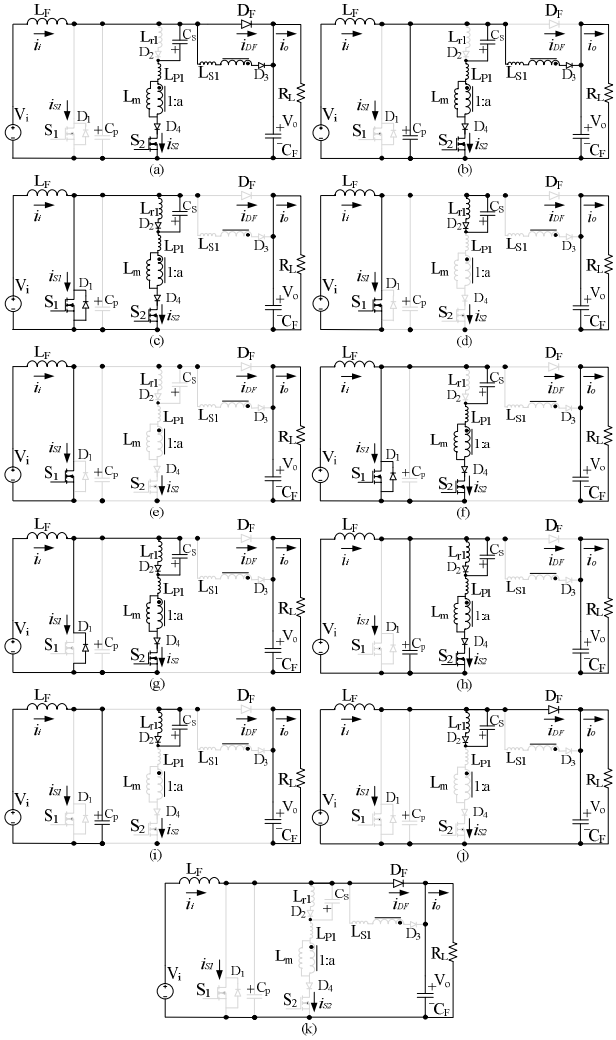

Fig. 2. Equivalent circuit schemes for operating stages

$$\omega_2 = \frac{1}{\sqrt{L_{r1}C_S}} \tag{17}$$

$$Z_1 = \sqrt{\frac{L_{r1}}{C_S}} \tag{18}$$

At $t = t_5$, the voltage of C_s reaches maximum value and the current of L_{r1} falls zero. Then, this stage ends.

$$v_{CS\max} = \sqrt{{V_{CS4}}^2 + \left(Z_1 I_{Lr14}\right)^2} \tag{19}$$

In here, V_{CS4} and I_{Lr14} are the values of V_{CS} and I_{Lr1} at the end of Stage 4.

Stage 5 [$t_5 < t < t_6$: Fig. 2(e)]

This stage is basic PWM boost converter on–state stage and the main switch S_1 passes the input current I_i. At $t = t_6$, the control signal is applied to the gate of the auxiliary switch S_2 and it is turned on with ZCS due to series inductance L_{lk}. Then, this stage ends.

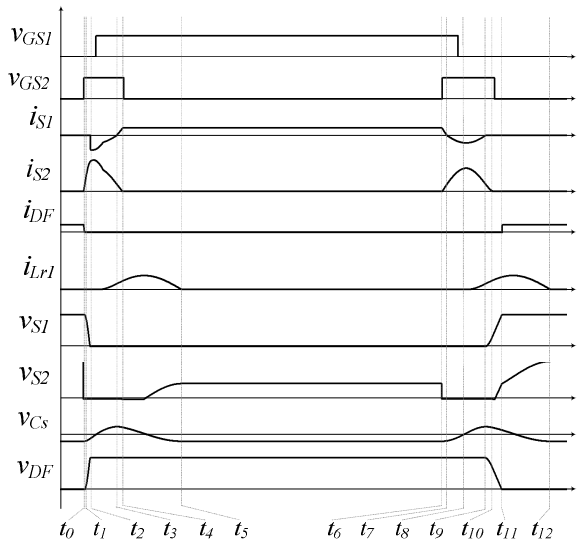

Fig. 3. Key waveforms concerning the operation stages in the proposed converter

Stage 6 [$t_6 < t < t_8$: Fig. 2(f)]

At $t = t_6$, a resonance starts between the snubber capacitor C_s and the transformer primary inductance after the auxiliary switch is turned on. The main switch current begins to decrease while the current of S_2 is increasing.

At $t = t_7$, the current of S_1 falls zero when the current of S_2 reaches I_i. Thus, D_1 turns on with ZCS and it conducts the current excess of input current. This stage is called ZCT stage where D_1 is in the on–state. The control signal of the main switch S_1 is removed in middle this stage. In this way, the main switch S_1 is turned off with ZCT. In here, the resonant inductance current i_{Lr2} and the resonant capacitor voltage v_{CS} can be expressed as follows:

$$v_{CS} = V_{CS\max}\cos\left(\omega_1\left(t-t_6\right)\right) \tag{20}$$

$$i_{Lr2} = \frac{V_{CS\max}}{Z_2}\sin\left(\omega_1\left(t-t_6\right)\right) \tag{21}$$

$$Z_2 = \sqrt{\frac{L_{r2}}{C_S}} \tag{22}$$

At $t = t_8$, the current of primary inductance i_{Lr2} reaches maximum value when the voltage of C_s falls zero. Then, this stage ends.

$$i_{Lr2\max} = \frac{V_{CS\max}}{Z_2} \tag{23}$$

Stage 7 [$t_8 < t < t_9$: Fig. 2(g)]

At $t = t_8$, a new resonance starts via $L_{r1} - L_{r2} - C_s$ and the energy of the transformer primary inductance is transferred to L_{r1} and C_s. In here, the resonant inductance currents i_{Lr1}, i_{Lr2} and the resonant capacitor voltage v_{CS} can be expressed as follows:

$$v_{CS} = \frac{I_{Lr2}}{\omega_e C_S}\sin\left(\omega_e\left(t-t_8\right)\right) \tag{24}$$

$$i_{Lr1} = \frac{L_e}{L_{r1}} I_{Lr2\max}\left(1-\cos\left(\omega_e\left(t-t_8\right)\right)\right) \tag{25}$$

$$\begin{aligned} i_{Lr2} &= \frac{L_e}{L_{r1}} I_{Lr2\max}\left(1-\cos\left(\omega_e\left(t-t_8\right)\right)\right) \\ &+ I_{Lr2\max}\left(1-\cos\left(\omega_e\left(t-t_8\right)\right)\right) \end{aligned} \tag{26}$$

At $t = t_9$, D_1 turns off when the current of primary inductance falls I_i and this stage ends.

Stage 8 [$t_9 < t < t_{10}$: Fig. 2(h)]

In this stage, a resonance occurs between C_p and snubber cell with the constant input current. The current of L_{r1} increases while the current of transformer primary inductance decreases. For this stage

$$L_{r1}\frac{di_{Lr1}}{dt} = V_{CS} \tag{27}$$

$$L_{r2}\frac{di_{Lr2}}{dt} = V_{Cp} - V_{Cs} \tag{28}$$

$$C_S\frac{dv_{CS}}{dt} = i_{Lr2} - i_{Lr1} \tag{29}$$

$$C_p\frac{dv_{Cp}}{dt} = I_i - i_{Lr2} \tag{30}$$

equations are valid. At $t = t_{10}$, the current of primary inductance falls zero and the control signal of S_2 is removed. So, S_2 turns off with ZCS and this stage ends.

Stage 9 [$t_{10} < t < t_{11}$: Fig. 2(i)]

In this stage, two discrete circuits occur. The parasitic capacitor C_p is linearly charged with the constant input current and the energy stored in L_{r1} is transferred to the C_s with resonance. For this stage

$$v_{CS} = V_{CS10}\cos\left(\omega_2\left(t-t_{10}\right)\right) - Z_1 L_{r110}\sin\left(\omega_2\left(t-t_{10}\right)\right) \tag{31}$$

$$i_{Lr1} = I_{Lr110}\cos\left(\omega_2\left(t-t_{10}\right)\right) + \frac{V_{CS10}}{Z_1}\sin\left(\omega_2\left(t-t_{10}\right)\right) \tag{32}$$

$$v_{Cp} = \frac{I_i}{C_p}\left(t-t_{10}\right) \tag{33}$$

equations are valid. At $t = t_{11}$, the voltage of C_p reaches the output voltage and so, the main diode D_F is turned on with ZVS. Then, this stage ends.

Stage 10 [$t_{11} < t < t_{12}$: Fig. 2(j)]

In this stage, the resonance between L_{r1} and C_s continues. All energy of L_{r1} is transferred to C_s during this stage. For this stage

$$v_{CS} = V_{CS11}\cos\left(\omega_2\left(t-t_{11}\right)\right) - Z_1 L_{r111}\sin\left(\omega_2\left(t-t_{11}\right)\right) \tag{34}$$

$$i_{Lr1} = I_{Lr111}\cos\left(\omega_2\left(t-t_{11}\right)\right)+\frac{V_{CS11}}{Z_1}\sin\left(\omega_2\left(t-t_{11}\right)\right) \quad (35)$$

$$v_{Cp} = \frac{I_i}{C_p}\left(t-t_{11}\right) \quad (36)$$

equations are valid. At $t = t_{12}$, the current of L_{r1} falls zero and this stage ends.

Stage 11 [$t_{12} < t < t_{13} = t_0$: Fig. 2(k)]

In this stage, the main diode D_F is in the on–state and conducts the input current. This stage is basic PWM boost converter off–state stage. Thus, it is returned to initial conditions and the stages expressed are repeated in the next switching cycle.

3. Design procedure

In this section, the design procedure of the proposed converter is presented.

The time that the resonance inductance current reaches maximum input current should be smaller than auxiliary switch rise time (t_{rS2}) for turning on the auxiliary switch with ZCS.

$$\frac{V_o + V_{CS\max}}{L_{r2}} t_{rS2} \le I_i \quad (37)$$

The value of L_{r1} inductance should be twice of the value of L_{r2} inductance for turning off the auxiliary switch with ZCS.

$$L_{r1} \ge 2L_{r2} \quad (38)$$

The transformer secondary turns N_2 should be between 1–1.5 times of the primary turns N_1. Since the energy transferred to the output falls at higher turn rates.

$$N_1 \le N_2 \le 1.5N_1 \quad (39)$$

C_p capacitor is sum of the parasitic capacitors of the main switch and the main diode.

The duration of t_{ZVT} should be longer than the main switch rise time (t_{rS1}) in order to turn on the main switch with ZVT.

$$t_{rS1} \le t_{ZVT} \quad (40)$$

The duration of t_{ZCT} should be longer than the main switch fall time (t_{fS1}) in order to turn off the main switch with ZCT.

$$t_{fS1} \le t_{ZCT} \quad (41)$$

Table 1. The experimental parameters and the device values of proposed converter

Output Power (P_o)	500 W	Snubber Inductance (L_{r1})	5 µH
Frequency (f_s)	100 kHz	N_1:N_2= 1:a	1:1.5
Input Voltage (V_{acrms})	220 V	Snubber Capacitor (C_S)	22 nF
Output Voltage (V_o)	400 V	Parasitic Capacitor (C_p)	1.5 nF
Main Inductance (L_F)	1mH	Output Capacitor (C_F)	470 µF

Table 2. Some significant values of the semiconductor elements used in the prototype converter

Devices	Part Number	V (V)	I (A)	t_{rr} (ns)
S_1	IXFH30N60P	600	30	200
S_2	FCP190N60E	600	20	308
D_F	MUR860	600	8	60
D_2, D_3, D_4	DESI8-06	600	8	50

4. Experimental Results

The experimental prototype of the proposed converter was implemented with reference to the parameters in Table 1. Besides, the semiconductor devices used in the experimental prototype are given in Table 2.

Fig. 4 shows the experimental results of the proposed converter. These results are compatible with theoretical analysis. In Fig. 4(a), the current and voltage waveforms of the main switch are illustrated. As shown in the figure, the main switch is turned on with ZVT without the current and voltage overlapping. Moreover, the main switch is turned off with ZCT. Therefore, the turning on switching power losses is eliminated by ZVT and the turning off switching power losses is eliminated by ZCT. Besides, there is no extra voltage and/or current stress on the main switch.

In Fig. 4(b), the current and voltages waveforms of the main diode are illustrated. The main diode is turned on with ZVS and turned off with ZCS. So, its switching power losses and reverse recovery losses are significantly reduced. Moreover, there is no extra voltage or current stress on the main diode.

In Fig. 4(c), the current and voltage waveforms of the auxiliary switch are illustrated. As shown in figure, the auxiliary switch is turned on and off with ZCS. Therefore, the turning on and off switching power losses is reduced for the auxiliary switch. Additionally, the extra voltage stress of the auxiliary switch is quite low.

In Fig. 4(d), the input voltage and the input current waveforms are illustrated for operating 220 V input voltage and 50 Hz frequency. The experimental measured power factor is 99.7% and THD is 3.9% for 220 V input voltage at full load. Besides, the varying of power factor depend on different line voltage is illustrated in Fig. 5.

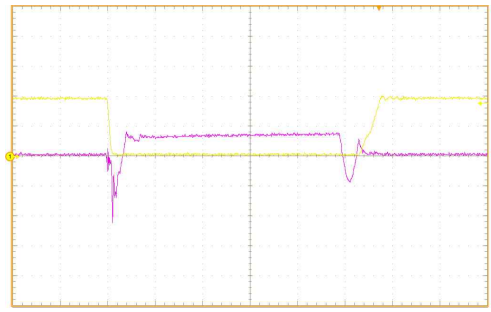

(a)

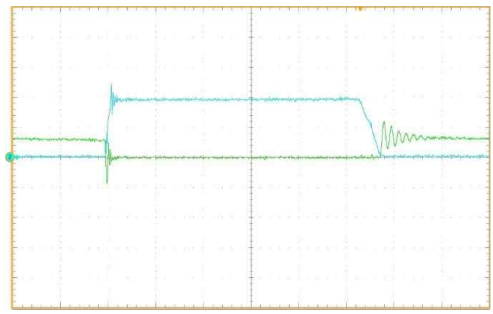

(b)

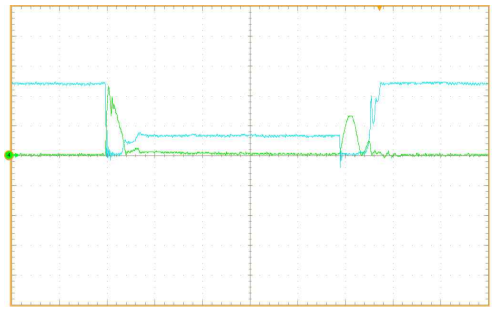

(c)

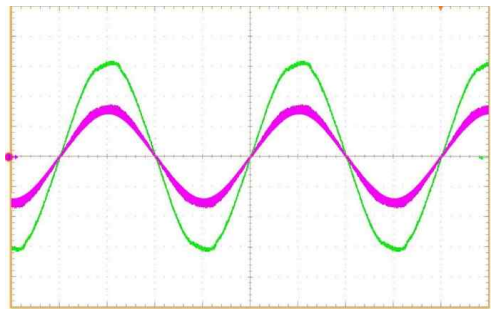

(d)

Fig. 4. Experimental results of current and voltage waveforms of (a) S1, (b) DF, (c) S2 (200 V/div, 10 A/div, 2 μs/div), and (d) voltage and current waveform of the line (100 V/div, 2 A/div, 5 ms/div)

The efficiency graphics of the proposed converter and HS converter are illustrated in Fig. 6. While the efficiency value of converter is about 93% by hard switching, it is measured 97.1% for soft switching at the nominal output power.

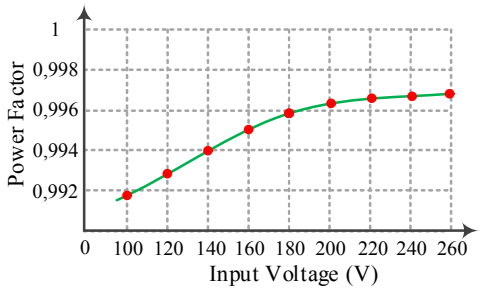

Fig. 5. Power factor depend on varying line voltage

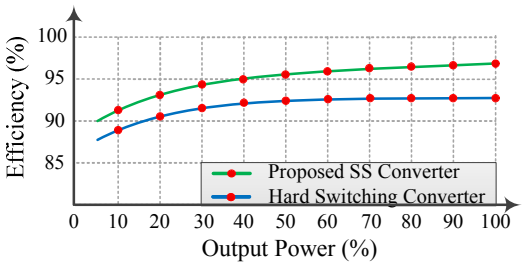

Fig. 6. The efficiency curves of the proposed converter comparatively

5. Conclusion

In this paper, a novel SS PWM–PFC AC–DC boost converter is presented for PFC applications. The proposed snubber cell provides ZVT turning on and ZCT turning off for the main switch. Besides the main diode is turned on with ZVS and turned off with ZCS while all of auxiliary semiconductor devices are SS. The majority of switching energies is transferred to the output side by auxiliary transformer during ZVT operation. Thus, the current stress of the auxiliary switch significantly reduced. Furthermore, the proposed converter is operated wide input line voltage and output current range. The detailed theoretical analysis of novel converter has been done and this analysis has been verified by an experimental study with 100 kHz, 500 W.

References

[1] Sanjeev Singh and Bhim Singh, "PFC Bridge Converter for Voltage-controlled Adjustable-speed PMBLDCM Drive," *Journal of Electrical Eng. & Tech.*, vol. 6, pp. 215-225, Mar. 2011.

[2] Nihan Altintas, "A Novel Single Phase Soft Switched PFC Converter," *Journal of Electrical Eng. & Tech.*, vol. 9, no. 1592-1601, Sep. 2014.

[3] Yakup Sahin, Naim Suleyman. Ting and Ismail Aksoy, "A highly efficient ZVT–ZCT PWM boost converter with direct power transfer," *Electrical Engineering*, doi: 10.1007/s00202-017-0546-y.

[4] Naim Suleyman Ting, Yakup Sahin and Ismail Aksoy, "Analysis, Design and Implementation of a Zero-

Voltage-Transition Interleaved Boost Converter," *Journal of Power Electron.*, vol. 17, no. 1, pp. 41-55, Jan. 2017.
[5] Guicha Hua, Ching-Shan Leu, Yimin Jiang, F. C. Y. Lee, "Novel Zero-Voltage-Transition PWM Converters," *IEEE Trans. on Power Electron.*, vol. 9, pp. 213-219, Mar. 1994.
[6] Ching-Jung Tseng, Chern-Lin Chen, "Novel ZVT-PWM Converters with Active Snubbers," *IEEE Trans. Power Electron.*, vol. 13, no. 5, pp. 861-869, Sep. 1998.
[7] Paulo J. M. Menegaz, Marcio A. Co, Domingos S. L. Simonetti and Jose L. F. Vieira, "Improving the Operation of ZVT DC-DC Converters," *30th Power Electronics Specialist Conference*, vol. 1, pp. 293-297, Jul. 1999.
[8] K. Mark Smith and Keyue Ma Smedley, "Properties and Synthesis of Passive Lossless Soft-Switching PWM Converters," *IEEE Trans. Power Electron.*, vol. 14, no. 5, pp. 890-899, Sep. 1999.
[9] Doung-Yun. Lee, Byoung-Kuk. Lee, Sang-Bong Yoo and Dong-Seok Hyun, "An Improved Full-Bridge Zero-Voltage-Transition PWM DC/DC Converter with Zero-Voltage/Zero-Current Switching of the Auxiliary Switches," *IEEE Trans. Industrial Applications*, vol. 36, no. 2, pp. 558-566, Mar. 2000.
[10] Naim Suleyman Ting, Ismail Aksoy and Yakup Sahin, "ZVT-PWM DC-DC Boost Converter with Active Snubber Cell," *IET Power Electronics*, vol. 10, no. 2, pp. 251-260, Feb. 2017.
[11] Oliver Stein, Helio L. Hey, "A True ZCZVT Commutation Cell for PWM Converters," *IEEE Trans. on Power Electron.*, vol. 15, pp. 185-193, Jan. 2000.
[12] Sungsik Park, Yohan Park, Sewan Choi, Woojin Choi and Kyo-Beum Lee, "Soft-Switched Interleaved Boost Converters for High Step-Up and High-Power Applications," *IEEE Trans. on Power Electron.*, vol. 26, pp. 2906-2914, Oct. 2011.
[13] Serkan Dusmez, Alireza Khaligh, Amin Hasanzadeh, "A Zero-Voltage-Transition Bidirectional DC/DC Converter," *IEEE Trans. on Industrial Electron.*, vol. 62, pp. 3152-3162, May 2015.
[14] Haci Bodur, A. Faruk Bakan, "A New ZVT-PWM DC-DC Converter," *IEEE Trans. on Power Electron*., vol. 17, pp. 40-47, Jan. 2002.
[15] Ranganathan Gurunathan and Ashoka K. S. Bhat, "A Zero-Voltage Transition Boost Converter Using a Zero-Voltage Switching Auxiliary Circuit," *IEEE Trans. on Power Electron.,* vol. 17, pp. 658-668, Sep. 2002.
[16] Yie-Tone Chen, Shin-Ming Shiu and Ruey-Hsun Liang "Analysis and Design of a Zero-Voltage-Switching and Zero-Current-Switching Interleaved Boost Converter," *IEEE Trans. on Power Electron.*, vol. 27, pp. 161-173, Jan. 2012.
[17] Nihan Altintas, A. Faruk Bakan and Ismail Aksoy "A Novel ZVT-ZCT-PWM Boost Converter," *IEEE Trans. on Power Electron.*, vol. 29, pp. 256-265, Jan. 2014.
[18] Ismail Aksoy, Haci Bodur, A. Faruk Bakan "A New ZVT-ZCT-PWM DC-DC Converter," *IEEE Trans. on Power Electron.*, vol. 25, pp. 2093-2105, August 2010.
[19] Satilmis Urgun, "Zero-Voltage Transition Zero-Current Transition Pulsewidth Modulation DC-DC Buck Converter with Zero-Voltage Switching Zero-Current Switching Auxiliary Circuit," *IET Power Electron.*, vol. 5, pp. 627-634, Nov. 2011.
[20] Pritam Das, Gerry Moschopoulos "A Comparative Study of Zero-Current-Transition PWM Converters," *IEEE Trans. on Industrial Electron*., vol. 54, pp. 1319-1328, Jun. 2007.
[21] Haci Bodur and A. Faruk Bakan "A New ZVT-ZCT-PWM DC-DC converter," *IEEE Transactions on Power Electron.*, vol. 19, pp. 1919-1926, May 2004.
[22] Naim Suleyman Ting, Yakup Sahin and Ismail Aksoy "A ZVT-ZCT-PWM DC-DC boost converter with direct power transfer" *World Academy of Science, Engineering and Technology International Journal of Electrical, Computer, Energetic, Electronic and Communication Engineering* vol. 10, no. 5, pp. 671-676, 2016.

Yakup Sahin received the Ph.D. degree from Yildiz Technical University, in 2016. Currently, he is Assist. Prof. in the Department of Electrical and Electronics Engineering, Bitlis Eren University, Turkey. His research interest is power electronics.